JOURNAL OF GUIDANCE, CONTROL, AND DYNAMICS
Vol. 34, No. 2, March–April 2011

Intercept-Angle Guidance

Tal Shima*
Technion—Israel Institute of Technology, Haifa 32000, Israel

DOI: 10.2514/1.51026

A new guidance concept is proposed. Implementing it enables intercepting a maneuvering target while also imposing, from early on in the engagement, a predefined angle relative to the target's velocity vector. The scenario of interest is aerial interception between a missile and a maneuvering target. The guidance concept is applicable in all aerial interception geometries: namely, head-on, tail-chase, and the novel head-pursuit. Analytical conditions for existence of these different engagement geometries are derived. The guidance concept is implemented using the sliding-mode approach. The common assumption of flight along an initial collision triangle is not taken, and thus the guidance law is applicable for both midcourse and endgame guidance. The application in the different engagement geometries is studied via simulation. It is shown that the head-on scenario allows the smallest range of intercept angles. It also places the most severe maneuverability requirements on the interceptor. Thus, in some cases, tail-chase or head-pursuit engagements should be considered instead. The choice between the two is dependent on the adversary's speed ratio; for tail-chase, the interceptor must have a speed advantage over its target, while for head-pursuit, it must have a speed disadvantage.

I. Introduction

GUIDANCE of autonomous vehicles is usually concerned with reaching a moving point in space. Application areas are on land, in sea, in air, and in space. Here, we deal with a generic aerial interception problem in which a missile chases a maneuvering target. The scenarios of interest are the classical head-on (HO) and tail-chase (TC) scenarios, as well as the novel head-pursuit (HP) engagement presented in [1]. In HO the adversaries fly toward each other; in TC the interceptor chases the target; and in HP an interceptor with a speed disadvantage is positioned ahead of the target such that both fly in the same direction, with the target closing in on the interceptor (see Fig. 1). HO and TC are well-studied interception problems. In contrast, HP was conceived only recently, mainly to address the problem of intercepting high-speed targets such as ballistic missiles. In an HO engagement against such targets the closing speed is very high, imposing severe requirements on the interceptor systems, such as precise detection of the target from a large distance by the onboard seekers and very fast response time of the missile subsystems. To reduce the closing speed, TC can be used instead, but this requires a speed advantage from the interceptor. In HP the closing speed can be significantly reduced (compared to HO) without the need for a speed advantage, as in TC.

In such future interception scenarios it may be necessary to not just intercept the target, but to also achieve the interception with a predetermined angle relative to the target's flight path. This requirement may be due to several reasons: for example, a specific requirement on the hit angle for destroying the target's warhead, a special directional kill mechanism of the interceptor missile, observability considerations in noise-corrupted scenarios, and the target's capability to effectively employ countermeasures to various bearings (i.e., counter-countermeasures considerations).

Guidance laws are usually derived by assuming small deviations from a collision course allowing linearization [2]. Optimal control and differential games theory can be used for the derivation [2,3]. Proportional navigation (PN) [4] represents such a guidance law. Using such guidance laws and given that the assumption of small deviations from a collision course holds, the intercept angle relative to the target flight path is specified based on the initial collision triangle. In contrast, some classical guidance laws, such as pure pursuit (PP) and its derivative, deviated PP (DPP) [5], have been derived without assuming small deviations from a collision course. These guidance laws can impose a specific final interception geometry. In PP the interceptor is aimed at the target and it is intercepted from the rear [6]. The DPP guidance law is an extension of PP in that the missile is aimed at a constant lead angle to the target and it is intercepted from a constant angle, dependent on the lead angle and speed ratio [5]. A drawback of using these guidance laws is that they impose severe maneuver requirements on the interceptor. Moreover, they require a speed advantage from the interceptor and thus cannot be implemented, for example, in the HP engagement.

Variations of PN can be used in order to impose a predefined interception angle. Reference [7] presented an impact-angle-biased PN guidance law against a moving target. The PN line-of-sight (LOS) rate was extended with a time-varying component, and it was shown through simulation that acceptable performance can be obtained against slowly maneuvering targets. A recent paper [8] showed that varying the value of the PN navigation gain enables interception of a stationary target from various angles.

Optimal control theory can also be used to derive guidance laws that enforce an impact angle as well as a small miss distance. In [9] an optimal control guidance law was derived for imposing an intercept angle in a scenario in which a reentry vehicle pursues a fixed or slowly moving ground target. In [10] an optimal guidance law for intercept-angle control with a vehicle having a varying velocity was proposed. A constant, relatively low, target maneuver and a small initial heading error were assumed. The resulting guidance law required extensive information, including the perpendicular position and speed relative to the terminal heading and the target's path angle and angular rate. In [11] an optimal control law for a missile with arbitrary-order dynamics launched against a stationary target was derived. Reference [12] extends the same formulation by adopting a time-to-go weighted-energy cost function. Explicit guidance [13] was recently used to enforce an impact angle [14]. It was shown that the guidance law can simultaneously achieve design specifications on miss distance and final missile-target relative orientation. The guidance law is parameterized in terms of a design coefficient that determines the degree of curvature in the trajectory.

Imposing an impact angle can also be performed by a circular navigation guidance law [15]. The name of this guidance law stems from the imposed approach path along an arc of a circle toward the target. One limitation though of this guidance law is the need for an interceptor speed advantage, and thus, as in PP and DPP mentioned

Presented as Paper 2007-6782 at the AIAA Guidance, Navigation, and Control Conference, Hilton Head, SC, 20–23 August 2007; received 3 June 2010; revision received 6 September 2010; accepted for publication 7 September 2010. Copyright © 2010 by the author. Published by the American Institute of Aeronautics and Astronautics, Inc., with permission. Copies of this paper may be made for personal or internal use, on condition that the copier pay the $10.00 per-copy fee to the Copyright Clearance Center, Inc., 222 Rosewood Drive, Danvers, MA 01923; include the code 0731-5090/11 and $10.00 in correspondence with the CCC.

*Senior Lecturer, Department of Aerospace Engineering; tal.shima@technion.ac.il. Associate Fellow AIAA.

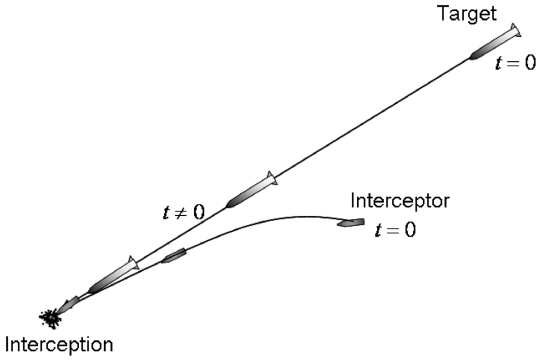

Fig. 1 Head-pursuit engagement.

previously, it cannot be used in an HP scenario. A more complicated guidance law that can impose initial and final flight-path angles was introduced in [16]. The algorithm requires the solution of a two-point boundary-value problem and thus can be implemented against targets with known trajectories. In [17] a differential geometric guidance law was proposed that forces a side impact of the target, without relying on line-of-sight information.

Linear quadratic optimal control and differential games guidance laws that explicitly enable imposing a predetermined intercept angle against a maneuvering target were presented in a recent paper [18]. The obtained guidance laws were shown to be dependent on the well-known zero-effort miss distance and on a new variable, denoted as the zero-effort angle. For implementation in scenarios in which the engagement was not initiated on the required collision triangle, the state-dependent differential-Riccati-equation-like technique was used. In [19] the problem of imposing an intercept angle in a planar engagement scenario with a stationary target was investigated. A unique implementation of the state-dependent algebraic Riccati equation technique was used to solve the nonlinear regulator problem. Simulations confirmed the usefulness of the approach for various firing angles.

If flight along an initial collision triangle does not satisfy the requirement of the intercept angle, then the nonlinear interception problem can be analyzed using nonlinear control techniques, such as the sliding-mode control (SMC) methodology. This nonlinear robust control tool enables dealing with highly nonlinear systems with large modeling errors and uncertainties [20]. In SMC the controller is obtained by converting an nth-order tracking problem to a first-order stabilization problem. The design is performed around a sliding surface commonly denoted by $\sigma = 0$, where the sliding variable σ is a function of the system tracking error and possibly its derivatives. The number of derivatives used to define the sliding variable is dictated by the relative degree of the system. The problem is then to drive the scalar quantity defining the sliding surface to zero and maintain it there, ultimately achieving exact tracking. If the tracking error is confined to the chosen sliding surface, then the scalar error will decay to zero with desired dynamics and we say that the system is in sliding mode. The control action required for maintaining the system in sliding mode, obtained by imposing $\dot{\sigma} = 0$, is denoted as the equivalent control. Erroneous equivalent control values can be obtained as a result of system modeling inaccuracies, uncertainties, and disturbances, and as a result, the system may depart the sliding surface. To accommodate the inherent departures from the surface and also to initially bring the system to sliding mode, the equivalent control is augmented by an additional component, commonly denoted as the uncertainty control. This control, which is responsible for driving the system to the sliding surface in finite time while ensuring closed-loop stability, is derived while assuming knowledge only of the bounds on the inaccuracies, uncertainties, and disturbances.

The SMC methodology has been successfully used in various guidance applications. A missile guidance law in the class of PN, derived using the SMC approach, was proposed in [21]. The sliding surface was selected to be proportional to the LOS rate, and the target maneuvers were considered as bounded uncertainties. Using numerical simulations, the superiority of the proposed guidance law over the conventional PN was advocated. In [22] an adaptive sliding-mode guidance law was derived. Using analysis and simulations, robustness to disturbances and parameter perturbations was shown. In [23] a smooth second-order sliding-mode control-based guidance law was presented. In [24–26] traditional and high-order SMC was used to design an integrated autopilot-guidance loop for missiles with single and dual control surfaces. In a recent paper [1] SMC was applied to tailor a guidance law for the unique HP engagement, where the missile has a speed disadvantage.

In this paper we present a new guidance concept and implement it using SMC. The guidance law enables intercepting a maneuvering target while also imposing, from early on in the engagement, a predefined angle relative to the target's velocity vector. The guidance law is applicable in all aerial interception geometries: namely, head-on, tail-chase, and the novel head-pursuit. As flight along an initial collision triangle is not assumed in the derivation, the guidance law is suitable for both midcourse and endgame guidance.

In the next section the 2-D equations of motion of the problem are presented. Then, the different interception engagements are discussed and analyzed. Next, the guidance principle is proposed and the sliding-mode controller is derived. This is followed by a performance analysis of the guidance law in the different engagements. Concluding remarks are presented in the last section.

II. Equations of Motion

An engagement between an interceptor missile and a maneuvering target is analyzed. We assume that the motion of the interceptor can be separated into two perpendicular channels, and thus the guidance problem can be treated as planar in each of these channels (as is the case, for example, for a roll-stabilized endoatmospheric interceptor).

The planar endgame geometry, which can also represent other similar interception problems such as robot pursuit, is shown in Fig. 2. The target is denoted as T and the interceptor is denoted as I. The speed, maneuvering acceleration, and flight-path angle are denoted by V, a, and γ, respectively; the range between the target and interceptor is r, and λ is the LOS angle relative to a fixed reference. The angles θ and δ are, respectively, the target's and interceptor's directions of flight relative to the LOS.

We first assume that the interceptor and target speeds (V_I and V_T, respectively) are constant, and we define the nondimensional parameter K as the speed ratio:

$$K \triangleq V_I/V_T \tag{1}$$

We define the speeds along and perpendicular to the LOS as V_r and V_λ, respectively, satisfying

$$V_r = V_I \cos\delta - V_T \cos\theta \tag{2}$$

$$V_\lambda = V_I \sin\delta - V_T \sin\theta \tag{3}$$

Their time derivatives are

$$\dot{V}_r = a_T \sin\theta - a_I \sin\delta + V_\lambda^2/r \tag{4}$$

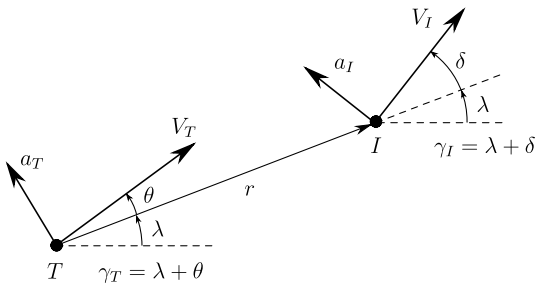

Fig. 2 Planar engagement geometry.

$$\dot{V}_\lambda = a_I^\perp - a_T^\perp - V_\lambda V_r / r \tag{5}$$

where $a_I^\perp$ and $a_T^\perp$, satisfying

$$a_I^\perp = a_I \cos\delta \tag{6}$$

$$a_T^\perp = a_T \cos\theta \tag{7}$$

are the interceptor and target acceleration components perpendicular to the LOS. We assume that during the scenario $\delta \neq \pi/2, 3\pi/2$, as in such singular cases the interceptor has no maneuver capability perpendicular to the LOS.

The engagement kinematics can now be expressed in a polar coordinate system (r, λ) attached to the target:

$$\dot{r} = V_r \tag{8}$$

$$\dot{\lambda} = V_\lambda / r \tag{9}$$

The missile and target accelerations, a_I and a_T, respectively, determine the interceptor and target trajectories:

$$\dot{\gamma}_I = a_I / V_I \tag{10}$$

$$\dot{\gamma_T} = a_T / V_T \tag{11}$$

where the flight-path angles γ_I and γ_T satisfy

$$\gamma_I = \lambda + \delta \tag{12}$$

$$\gamma_T = \lambda + \theta \tag{13}$$

From Eqs. (10–13) we obtain

$$\dot{\delta} = a_I / V_I - V_\lambda / r \tag{14}$$

$$\dot{\theta} = a_T / V_T - V_\lambda / r \tag{15}$$

We assume that the target's closed-loop dynamics can be represented by the following equivalent first-order transfer function:

$$\dot{a}_T = (a_T^c - a_T)/\tau_T + \Delta_T \tag{16}$$

where τ_T is the time constant, and a_T^c and Δ_T are the bounded acceleration command and modeling error, respectively.

III. Interception Engagements

In this section the three possible interception engagements are discussed. They are distinguished by their unique geometries. We first define these engagements and then provide conditions for their existence.

A. Definitions

We denote the running time as t. The engagement initiates at $t = 0$ with $\dot{r}(t = 0) < 0$ and terminates at $t = t_f$, where

$$t_f = \arg_t \{ r(t)\dot{r}(t) = 0 \} \tag{17}$$

The miss distance is $r(t_f)$.

Definition 1: Perfect intercept is an interception engagement with $r(t_f) = 0$.

It directly follows from Eq. (17) that in order to obtain perfect intercept, the following condition must be satisfied:

$$\dot{r}(t) < 0 \quad \forall\ r(t) > 0 \tag{18}$$

Next, we define the three possible interception engagements that are based on the relative geometry at the endgame, near the engagement termination at t_f.

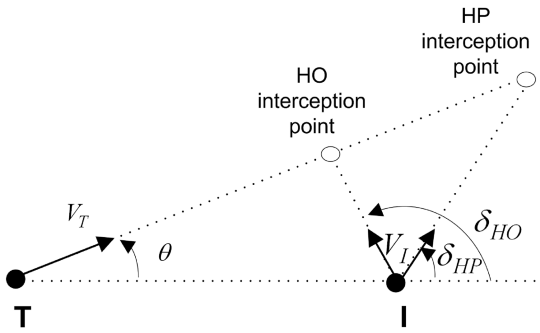

Fig. 3 Possible engagements for $K < 1$. Interceptor can choose between head-on and head-pursuit.

Definition 2: Head-on is an interception engagement, where $\exists v > 0$: $-\pi/2 \leq \theta(t) \leq \pi/2$, and $\pi/2 \leq \delta(t) \leq 3\pi/2$ for $t \in [v, t_f)$.

Definition 3: Tail-chase is an interception engagement, where $\exists v > 0$: $\pi/2 < \theta(t) < 3\pi/2$, and $\pi/2 < \delta(t) < 3\pi/2$ for $t \in [v, t_f)$.

Definition 4: Head-pursuit is an interception engagement, where $\exists v > 0$: $-\pi/2 < \theta(t) < \pi/2$, and $-\pi/2 < \delta(t) < \pi/2$ for $t \in [v, t_f)$.

B. Geometries

In Figs. 3–5 the possible interception geometries are plotted for different speed ratios. These geometries were obtained for constant speeds and nonmaneuvering adversaries, under the condition that $V_r(t) < 0\ \forall\ t \in [0, t_f)$. Figure 3 presents the HO and HP engagements that are possible when $K < 1$ (i.e., $V_I < V_T$). Provided that interception can be reached, the interceptor can select between HO and HP by choosing its flight direction relative to the LOS (the angle δ). In Fig. 4 the HO and TC engagements are drawn for the case in which $K > 1$. Here, the target's flight direction defines a unique engagement. For $K = 1$, then only HO (plotted in Fig. 5) is possible.

C. Conditions

Conditions for the existence of the different engagement geometries are given next. These conditions are derived under the assumption of constant adversaries' velocities; i.e., the vehicles follow straight lines (do not maneuver) and their speed is constant.

Lemma 1. Assuming that

$$\exists v > 0\text{: } a_T(t) = a_I(t) = \dot{V}_T = \dot{V}_I = 0\ \forall\ t \in [v, t_f)$$

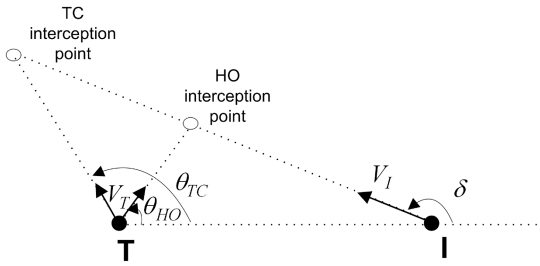

Fig. 4 Possible engagements for $K > 1$. Target's flight direction defines either head-on or tail-chase.

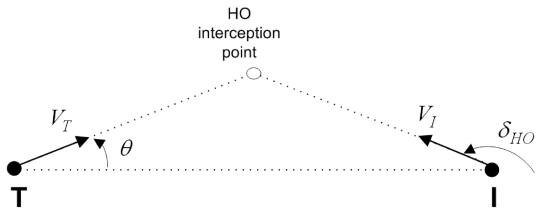

Fig. 5 Possible engagement for $K = 1$. Only head-on is feasible.

(i.e., the adversaries have constant velocities) and $V_r(v) < 0$, then a necessary and sufficient condition for perfect intercept [i.e., $r(t_f) = 0$] is that $V_\lambda(v) = 0$.

Proof of sufficient condition: If $V_\lambda(v) = 0$, then from Eqs. (2–5), $V_\lambda = \dot{V}_\lambda = \dot{V}_r = 0 \ \forall \ t \in [v, t_f)$. Consequently, $V_r(t) = V_r(v) < 0 \ \forall \ r(t) > 0$ and the engagement terminates with $r(t_f) = 0$. □

Proof of necessary condition: For perfect intercept to be achieved, then Eq. (18) must hold (i.e., $V_r(t) < 0 \ \forall \ r(t) > 0$). If $V_\lambda(v) > 0$, then from Eq. (5), $\dot{V}_\lambda(t) > 0 \ \forall \ t \in [v, t_f)$. Consequently, from Eq. (4), we obtain that $V_r = 0$ for $r > 0$ and Eq. (18) is not satisfied. By symmetry, the same holds for $V_\lambda(v) < 0$. For $V_\lambda(v) = 0$ Eq. (18) holds and the condition is proved. □

Remark 1: If the vehicles maneuver or have time-varying speeds, then in order to ensure interception, it is not required to enforce $V_\lambda(v) = 0$. Such is the case when an accelerating missile is chasing a constant-speed target and in order to implement guidance to collision (i.e., straight-line flight of the interceptor toward the predicted collision point) LOS rotation must be allowed [27].

Theorem 1: Given that $\exists v > 0$: $a_T(t) = a_I(t) = \dot{V}_T(t) = \dot{V}_I(t) = 0 \ \forall \ t \in [v, t_f)$ and $V_r(v) < 0$, then a necessary condition for perfect interception is

$$\begin{cases} |\sin(\theta(v))| \le K & K \le 1 \\ \theta(v) \text{ is arbitrary} & K > 1 \end{cases} \tag{19}$$

Proof: From Lemma 1, perfect intercept requires that $V_\lambda(v) = 0$. From Eq. (3), for $K \le 1$ this condition can be satisfied only if $|\sin(\theta(v))| \le K$. □

The necessary conditions on K, in order to obtain perfect intercept in HP or TC, are given in the next two theorems.

Theorem 2: Given that

$$\exists v > 0: \ a_T(t) = a_I(t) = \dot{V}_T(t) = \dot{V}_I(t) = 0 \ \forall \ t \in [v, t_f)$$

and $V_r(v) < 0$, a necessary condition for perfect interception in HP is $K < 1$.

Proof: Based on Lemma 1 and Definition 4, perfect HP interception requires that $\exists v > 0$: $V_\lambda(v) = 0$, $-\pi/2 < \theta(t) < \pi/2$, and $-\pi/2 < \delta(t) < \pi/2$ for $t \in [v, t_f)$. For $v > 0$, $V_r(v) < 0$, and $0 \le \theta(v) < \pi/2$, if $K \ge 1$, then in order to obtain $V_\lambda(v) = 0$, $\pi - \theta(v) \le \delta(v) \le \pi$ must be chosen. Consequently, as the vehicles are nonmaneuvering, $\pi/2 < \delta(t) \le \pi \ \forall \ t \in [v, t_f)$, terminating the engagement in HO. For $-\pi/2 < \theta(v) \le 0$ the condition is proved by symmetry. □

Theorem 3: Given that

$$\exists v > 0: \ a_T(t) = a_I(t) = \dot{V}_T(t) = \dot{V}_I(t) = 0 \ \forall \ t \in [v, t_f)$$

and $V_r(v) < 0$, a necessary condition for perfect interception in TC is $K > 1$.

Proof: Based on Lemma 1 and Definition 3, perfect TC interception requires that $\exists v > 0$: $V_\lambda(v) = 0$, $\pi/2 < \theta(t) < 3\pi/2$, and $\pi/2 < \delta(t) < 3\pi/2$ for $t \in [v, t_f)$. For $v > 0$, $V_r(v) < 0$, and $\pi/2 < \theta(v) \le \pi$, if $K \le 1$, then $\theta < \delta(v) \le \pi$ must be chosen. Consequently, $V_\lambda \ne 0 \ \forall \ t \in [v, t_f)$, and so perfect interception cannot be achieved. For $\pi \le \theta(t) < 3\pi/2$ the condition is proved by symmetry. □

The choices the interceptor has with regard to selecting the angle δ are dependent on the speed ratio K. These choices are provided next.

Theorem 4: Given $K < 1$ and that

$$\exists v > 0: \ a_T(t) = a_I(t) = \dot{V}_T(t) = \dot{V}_I(t) = 0 \ \forall \ t \in [v, t_f)$$

$V_r(v) < 0$, and $|\sin(\theta(v))| \le K$, then perfect interception can be ensured with two possible choices of δ. For $\pi/2 \le \delta(v) \le 3\pi/2$, HO is obtained; else, $-\pi/2 < \delta(v) < \pi/2$ and HP is obtained.

Proof: Given $K < 1$, then based on Theorem 3, perfect TC interception cannot be obtained. Based on Lemma 1, perfect intercept requires that $\exists v > 0$: $V_\lambda(v) = 0$. Given $K < 1$ and $|\sin(\theta(v))| \le K$, then in order to obtain $V_\lambda(v) = 0$, we must select $\delta(v) = \sin^{-1}[\sin(\theta(v))/K]$ [see Eq. (3)]. This equation has two solutions for δ, to be chosen by the interceptor. For $\pi/2 \le \delta(v) \le 3\pi/2$, based on Definition 2, the engagement is HO, and for $-\pi/2 < \delta(v) < \pi/2$, based on Definition 4, the engagement is HP. □

Theorem 5: Given $K = 1$ and that

$$\exists v > 0: \ a_T(t) = a_I(t) = \dot{V}_T(t) = \dot{V}_I(t) = 0 \ \forall \ t \in [v, t_f)$$

and $V_r(v) < 0$, $-\pi/2 < \theta(v) < \pi/2$, then perfect interception can be performed by a unique choice of angle δ. Using this choice the engagement is HO.

Proof: Given $K = 1$, then based on Theorems 2 and 3, HP and TC cannot be obtained. Given $-\pi/2 < \theta(v) < \pi/2$, then in order to satisfy $V_\lambda(v) = 0$ and $V_r(v) < 0$, we must select $\delta(v) = \pi - \theta(v)$ (see Eq. (3)) and the engagement is HO. □

Theorem 6. Given $K > 1$ and that

$$\exists v > 0: \ a_T(t) = a_I(t) = \dot{V}_T(t) = \dot{V}_I(t) = 0 \ \forall \ t \in [v, t_f)$$

and $V_r(v) < 0$, then perfect interception can be performed by a unique choice of δ. Using this choice, if $\pi/2 < \theta(v) < 3\pi/2$, then TC is obtained; or else, the engagement is HO.

Proof: Given $K > 1$, then based on Theorem 2, perfect HP interception cannot be obtained. Based on Lemma 1, perfect interception requires that $\exists v > 0$: $V_\lambda(v) = 0$. If $0 \le \theta(v) \le \pi/2$, then in order to satisfy $V_\lambda(v) = 0$ and $V_r(v) < 0$, then $\delta(v)$ must be chosen in the range $\pi - \theta < \delta(v) \le \pi$ and the target is intercepted in HO. If $\pi/2 < \theta(v) \le \pi$, then in order to satisfy $V_\lambda(v) = 0$ and $V_r(v) < 0$, $\delta(v)$ must be chosen in the range $\theta < \delta(v) \le \pi$ and the target is intercepted in TC. For $\pi < \theta(v) < 2\pi$ the condition is proved by symmetry. □

D. Regions

In Fig. 6 the conditions for the different interception regions are plotted as a function of the speed ratio K. Because of symmetry, the results are plotted only for $\theta \ge 0$. For $K < 1$ the allowable value of θ is obtained from Eq. (19). As stated in Theorem 4 and as is evident from Fig. 3, in such a case the choice between HO and HP interception is in the hands of the interceptor by the selection of the appropriate angle δ. For $K > 1$, as stated in Theorem 6 and as is evident from Fig. 4, the initial value of θ defines the engagement, either TC or HO. For $K = 1$, as stated in Theorem 5 and as is evident from Fig. 5, only HO is possible.

The corresponding values of δ as a function of θ that satisfy $V_\lambda = 0$ and $V_r < 0$, and consequently provide for perfect interception as long as the velocities of the opponents are constant, are plotted in Fig. 7. Because of symmetry, the results are plotted only for $0 \le \delta, \ \theta \le \pi$. Following Theorems 1 and 4, it is evident that if $K < 1$ and Eq. (19) is satisfied, then two solutions exist for equation $V_\lambda = 0$, providing either HO ($\pi/2 \le \delta \le \pi$) or HP ($0 \le \delta < \pi/2$) engagements. For $K = 1$, following Theorem 5, only HO ($0 \le \theta < \pi/2, \pi/2 < \delta \le \pi$) is possible. For $K > 1$, following Theorem 6, it is evident that for every choice of θ there exists a unique solution for δ. Based on

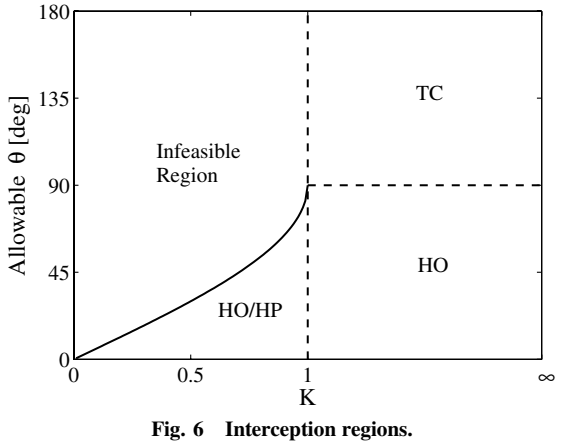

Fig. 6 Interception regions.

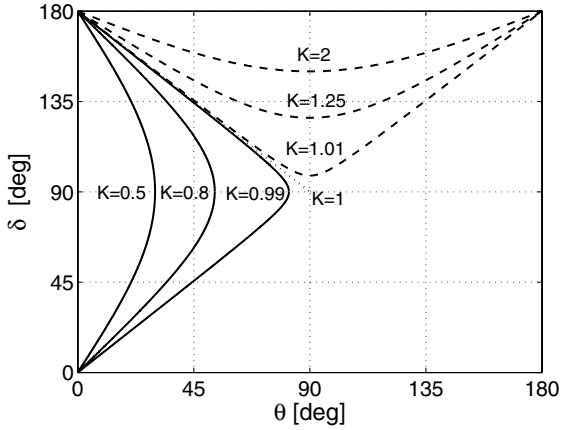

Fig. 7 Choice of δ as a function of θ for achieving interception.

Definitions 2 and 3 for $0 \le \theta \le \pi/2$, HO is achieved, and for $\pi/2 < \theta \le \pi$, it is TC.

IV. Guidance Concept

Our guidance objective is to obtain a predetermined intercept angle between the target velocity vector and the LOS. We denote this angle as θ_r. This is to be selected by the designer based on the interceptor's speed ability and the required interception geometry (HO, TC, or HP).

Assuming that the adversaries have constant speeds and that the target does not maneuver, then θ_r should be selected based on the results plotted in Fig. 6. As proved in the previous section, if the interceptor does not have a speed advantage (i.e., $K \le 1$), then there are restrictions on the selection of θ_r, whereas if the interceptor does have a speed advantage, there are no restrictions on the selection of θ_r.

For a feasible selection of θ_r, if the interceptor has a speed disadvantage (i.e., $K < 1$), then it can also select the intercept geometry, HO or HP, by its choice of the angle δ. For the case in which the interceptor does not have a speed disadvantage (i.e., $K \ge 1$), then the angle δ providing perfect intercept is unique.

To reach our guidance objective, i.e., $\theta(t_f^-) = \theta_r$, our new guidance concept will be to first reach $\theta = \theta_r$ at time v, where $0 < v < t_f$, and then enforce

$$\theta(t) = \theta_r \quad \forall\ t \in [v, t_f) \tag{20}$$

Thus, once the required angle θ is reached, we will seek to nullify the derivative of θ, i.e., to enforce

$$\dot{\theta}(t) = 0 \quad \forall\ t \in [v, t_f) \tag{21}$$

From Eq. (15), enforcing Eq. (21) results with an LOS rate that satisfies

$$\dot{\lambda} = \dot{\gamma}_T = a_T / V_T \tag{22}$$

If the target is not maneuvering, then this is equivalent to enforcing $\dot{\lambda} = 0$: i.e., maintaining the required collision triangle (with $\theta = \theta_r$) using the classical PN guidance. For a maneuvering or accelerating target, even after the intercept angle θ_r has been reached, these two guidance concepts differ, as Eq. (21) may be satisfied while $\dot{\lambda} \ne 0$. Specifically, for a constant-speed target, maintaining Eq. (21) [and, consequently, Eq. (22) is satisfied] and using Eq. (5) results with a missile acceleration perpendicular to the LOS, satisfying

$$a_I^{\perp} = 2V_r\dot{\lambda} + a_T^{\perp} + r\dot{a}_T/V_T \tag{23}$$

The first term on the right-hand side of Eq. (23) is equivalent to PN with a navigation constant of 2. The second term is required in order to match the current target maneuver. The third term is due to changes in the target maneuvers and it diminishes to zero as $r \to 0$. Note that maintaining Eq. (23) is required only after Eq. (20) has been satisfied: i.e., θ_r has been reached.

Deriving a guidance law that enforces the presented guidance concept in the face of initial errors (i.e., $\theta(0) \ne \theta_r$), target maneuvers, and modeling uncertainties falls naturally in the domain of sliding-mode control, as will be performed in the next section.

Remark 2: The proposed guidance concept does not entail the common assumption of flight along an initial collision triangle. Thus, it is applicable for both the midcourse and endgame phases of an interception engagement.

Remark 3: A unique feature of the proposed concept is that the required intercept geometry is enforced from early on in the scenario and not just at intercept. This may be advantageous from observability considerations (in noise-corrupted scenarios) and from counter-countermeasures considerations.

V. Sliding-Mode Guidance Law

In this section the SMC methodology is used to derive a guidance law based on the guidance concept presented in the previous section.

A. Sliding Variable

The objective of the guidance law is to enforce Eq. (20): i.e.,

$$\theta(t) = \theta_r \quad \forall\ t \in [v, t_f)$$

where $0 < v < t_f$ and θ_r is a constant chosen by the designer.

We define the deviation from the required intercept angle as

$$e = \theta - \theta_r \tag{24}$$

with its time derivatives being

$$\dot{e} = a_T/V_T - V_\lambda/r \tag{25}$$

$$\ddot{e} = [(a_T^c - a_T)/\tau_T + \Delta_T]/V_T - (\dot{V}_\lambda r - V_r V_\lambda)/r^2 \tag{26}$$

where V_r, V_λ, and $\dot{V}_\lambda$ are given in Eqs. (2), (3), and (5), respectively.

The relative degree of e with respect to the control command of the interceptor is denoted as rd and is equal to two as a_I appears only in $\ddot{e}$. To obtain a sliding variable σ with a relative degree of one, we define

$$\sigma = \left(\tau\frac{\mathrm{d}}{\mathrm{d}t} + 1\right)^{rd-1} e \tag{27}$$

where τ is the time constant selected such that the error e diminishes to zero at a required rate. Using this definition, we obtain

$$\sigma = \tau\dot{e} + e \tag{28}$$

Substituting Eqs. (24) and (25) in Eq. (28), we can write the sliding variable as

$$\sigma = (a_T/V_T - V_\lambda/r)\tau + \theta - \theta_r \tag{29}$$

Its time derivative is

$$\dot{\sigma} = \tau[(a_T^c - a_T)/\tau_T + \Delta_T]/V_T - \tau(a_I^{\perp} - a_T^{\perp} - V_\lambda V_r/r)/r + \tau V_r V_\lambda/r^2 + a_T/V_T - V_\lambda/r \tag{30}$$

B. Equivalent Controller

The sliding-mode controller $a_I^{\perp}$ consists of an equivalent part denoted as $a_{I\text{eq}}^{\perp}$ and an uncertainty part denoted as $a_{I\text{uc}}^{\perp}$, where

$$a_I^{\perp} = a_{I\text{eq}}^{\perp} + a_{I\text{uc}}^{\perp} \tag{31}$$

The equivalent controller is designed to maintain the system on the sliding surface, by imposing $\dot{\sigma}_0 = 0$ in the absence of modeling errors and target maneuver commands:

$$a_{I\text{eq}}^{\perp} = \arg_{a_I^{\perp}}\{\dot{\sigma}_0 = 0\} \tag{32}$$

where $\dot{\sigma}_0$ denotes the sliding variable time derivative with zero uncertainty (i.e., no target maneuver and modeling error). From Eq. (30), we obtain

$$\dot{\sigma}_0 = \dot{\sigma}(a_T^c = \Delta_T = 0) = \frac{a_T}{V_T}(1 - \tau/\tau_T + V_T\tau\cos\theta/r) - \frac{V_\lambda}{r}(1 - 2\tau V_r/r) - a_I^{\perp}\tau/r \tag{33}$$

Consequently, the obtained equivalent controller satisfies

$$a_{I\text{eq}}^{\perp} = 2V_r\dot{\lambda} + a_T^{\perp} - ra_T/(V_T\tau_T) + (ra_T/V_T - V_\lambda)/\tau \tag{34}$$

Note that the first three terms on the right-hand side of Eq. (34) are equivalent to those appearing in Eq. (23), while the remaining two terms diminish once $\dot{\theta} = 0$.

C. Uncertainty Controller

The system may not initially be in sliding mode. Or modeling errors and target maneuvers can cause the system to depart from the sliding surface, based on the following sliding variable dynamics obtained when using the controller of Eq. (31) with the equivalent controller of Eq. (34):

$$\dot{\sigma} = g - \tau a_{I\text{uc}}^{\perp}/r \tag{35}$$

where

$$g = \tau(a_T^c/\tau_T + \Delta_T)/V_T \tag{36}$$

The uncertainty controller is designed to drive the system, in finite time, to the sliding surface in face of uncertainties. The design of the uncertainty controller is based on the model of the target dynamics and the known bounds on the uncertainties. Note from Eq. (35) that as the range r gets smaller, the control authority of the interceptor increases.

Traditional sliding-mode control can be used for the derivation, yielding the following bang–bang controller:

$$a_{I\text{uc}}^{\perp} = R'\text{sgn}\sigma \tag{37}$$

To ensure convergence to the sliding surface R' is selected such that $R' > rg_{\max}$, where $g_{\max}$ is the bound on the uncertainty g (i.e., $|g| \le g_{\max}$). To avoid excessive chattering due to the discontinuous command of the uncertainty controller in Eq. (37), the SMC-based guidance law can be implemented with a boundary layer around the sliding surface:

$$a_{I\text{uc}}^{\perp} = R'\text{sat}(\sigma, \sigma_{\text{bl}}) \tag{38}$$

where $\text{sat}(\cdot,\cdot)$ is the standard saturation function and σ_{bl} is the width of the boundary layer around the sliding surface σ. Implementing this boundary layer compromises exact tracking by uniform ultimate boundedness of the tracking error [28].

Instead of traditional SMC, high-order sliding mode can be used in order to smooth out the interceptor's acceleration [23,26,29,30]. For example, a supertwisting second-order sliding-mode controller of the form [26]

$$a_{I\text{uc}}^{\perp} = r[-\alpha_1|\sigma|^{0.5}\text{sgn}(\sigma) + w]/\tau \tag{39}$$

$$\dot{w} = -\alpha_2\text{sgn}(\sigma) \tag{40}$$

can be used to obtain a continuous controller that drives the sliding variable σ and its derivative $\dot{\sigma}$ to zero in finite time in the presence of bounded disturbance $|\dot{g}| \le L$ [26]. Based on [29] the gains α_1 and α_2 can be selected as $\alpha_1 = 1.5\sqrt{L}$ and $\alpha_2 = 1.1L$. Note that third-order SMC can be used to obtain a continuous, as well as smooth, controller.

Table 1 Simulation parameters

Missile	Target	Kinematics
$V_I \in \{800, 1000, 2000\}$ m/s	$V_T = 1000$ m/s	$r(0) = 15$ km
$\delta(0) \in \{0, 180\}$ deg	$\theta(0) \in \{0, 180\}$ deg	$\lambda(0) = 0$ deg
$\sigma_{\text{bl}} = 1$ deg	$\tau_T = 0.1$ s	——
$\tau = 0.01$ s	$a_T \in \{0, 5\}$ g	——
——	$\Delta_T = 0$	——

D. Implementation Issues

The required information for the implementation of the guidance law, composed of the equivalent controller of Eq. (34) and an uncertainty controller such as that given in Eq. (38) or Eq. (39), is the varying values of r, δ, θ, V_λ, and a_T and the constants τ, θ_r, V_T, and τ_T. By using a radar seeker and an inertial navigation system, r and δ can be directly measured, whereas V_T, θ, V_λ, and a_T must be estimated. The constants τ and θ_r are design parameters, and the target's acceleration time constant τ_T is assumed known (otherwise, it may be estimated or used as a tuning parameter). Note that time-to-go is not needed for the implementation of this SMC guidance law, as the guidance objective is to reach the sliding surface $\sigma = 0$ in a given finite time.

Comparing this guidance law to the classical PN, a few observations can be made. First, the proposed guidance law does not necessarily yield a zero control command when $V_\lambda = 0$: e.g., if the guidance objective of $\theta = \theta_r$ has not yet been reached. Second, implementing this guidance law requires much more information, as PN requires only knowledge of $\dot{\lambda}$. Finally, the obtained guidance law is nonlinear, whereas PN is linear, thus forfeiting some analysis tools, such as the adjoint analysis.

VI. Simulation Analysis

In this section the implementation of the proposed guidance concept, which enforces a required intercept angle θ_r in perfect information HO, TC, and HP engagements, is studied using simulations. The simulation parameters are given in Table 1. For the sake of simplicity, the classical uncertainty controller of Eq. (38) was used. The initial conditions for the different engagements are as follows: for HO $\theta(0) = 0$ and $\delta(0) = 180$ deg, for HP $\theta(0) = 0$ and $\delta(0) = 0$, and for TC $\theta(0) = 180$ deg and $\delta(0) = 0$.

First, we investigate sample representative scenarios with a given value of intercept angle θ_r. Next, we investigate the ability of the guidance law to enforce a range of interception angles for scenarios with a nonmaneuvering target. Then, scenarios with a target performing a constant-5 g maneuver are investigated. For comparison, we also examine these scenarios using a pure proportional navigation guidance (PNG) law with a navigation constant of 4.

A. Sample Scenario

Figure 8 presents the interceptor and target trajectories in an inertial coordinate system for sample TC, HO, and HP engagements. In these engagements the speed of the interceptor was 2000, 1000, and 800 m/s, respectively. The initial locations of the missile and target for the three scenarios are identical and are marked by a square

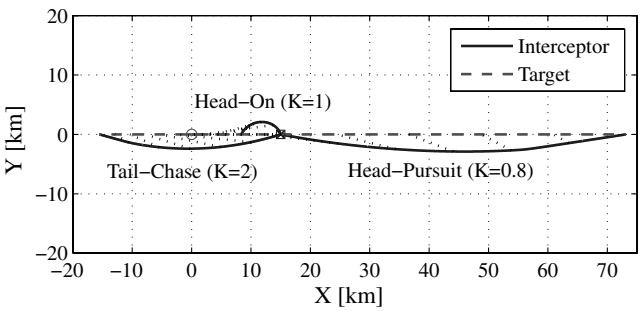

Fig. 8 Sample trajectories for head-pursuit, head-on, and tail-chase scenarios; target does not maneuver; $K \in \{0.8, 1, 2\}$.

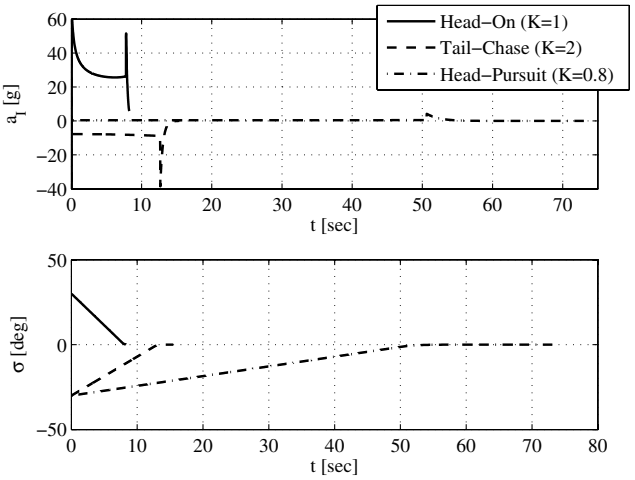

Fig. 9 Acceleration profiles and convergence to sliding surface for head-pursuit, head-on, and tail-chase scenarios; $K \in \{0.8, 1, 2\}$.

for the missile and by a circle for the target. In the HO and HP engagements, the velocity vector of the target is initially pointed toward the missile, while for TC it is pointed away. The requirement in these runs was for a deviation of 30 deg from the initial value of θ; i.e., the requirement on θ_r for TC, HO, and HP was 210, -30, and 30 deg, respectively. In all runs the LOS (plotted at several time instants and marked by a dotted line) initially rotates, until the required interception geometry is reached.

Figure 9 presents the missile acceleration profile (top frame) and convergence to the sliding surface (bottom frame) in the above three scenarios. The initial deviation in these runs of ± 30 deg from the sliding surface $\sigma = 0$ is evident. In the case of HO the surface is reached only very close to the termination point, while for the two other scenarios it is reached earlier. Note the difference in the scenario duration, due to the different interception geometries and interceptor's speed (HO: $t_f = 8.3$ s, HP: $t_f = 73.1$ s, and TC: $t_f = 15.5$ s).

Because of the long duration of the HP engagement, a small gain R' was chosen. Consequently, the acceleration requirement from the interceptor is the smallest and the convergence to the sliding surface is the slowest. The small acceleration requirement when using HP can also be attributed to the lowest interceptor speed in this engagement ($V_I = 800$ m/s). In contrast, HO requires the largest acceleration capability due to the geometry of the scenario imposing a very short engagement.

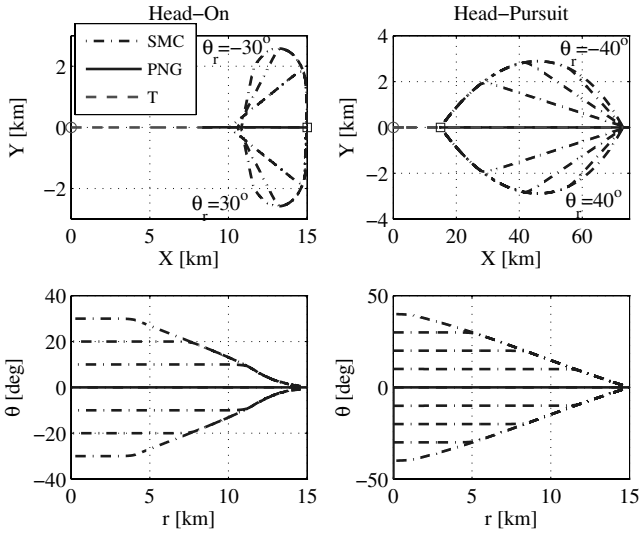

Fig. 10 Head-on and head-pursuit trajectories; target does not maneuver; $K = 0.8$.

Because of the boundary-layer implementation, chattering is avoided. The peaks in the accelerations occur when the sliding surface is reached. Choosing a larger boundary layer can eliminate this phenomenon, but may produce unsatisfactory guidance performance.

B. Nonmaneuvering Target

Figures 10–12 present the simulation results for varying requirements on the intercept angle θ_r. The target is assumed nonmaneuvering and three different speed ratios ($K = 0.8$, 1, and 2) are investigated.

Figure 10 presents the trajectories for the case in which the missile has a speed disadvantage ($K = 0.8$) and hence, based on Theorem 4, only head-on and head-pursuit are feasible. The two frames on the left present the head-on trajectories, while the frames on the right present those of head-pursuit. The top two frames present the trajectories in the Cartesian reference frame X–Y (note the different scaling in the X and Y axes). The two bottom frames present the relative trajectories in the polar coordinate system $\theta - r$ attached to the target. In all frames, multiple trajectories are plotted corresponding to a different requirement on the intercept angle θ_r (with an increment of 10 deg).

It is evident from Fig. 10 that using the proposed SMC guidance law enables interception of the target with different requirements for the angle between the LOS and the target's velocity vector: i.e., θ_r. Note that this angle is enforced from early on in the scenario and not just at intercept. For HO θ_r can vary between -30 and 30 deg, while for HP it can vary between -40 and 40 deg. The larger possible range of intercept angles while in an HP scenario can be attributed to the longer interception duration due to the considerably smaller closing speed (approximately 200 m/s in HP, compared to approximately 1800 m/s in HO). The symmetry for positive and negative values of θ_r is also clearly evident and is attributed to the constant-heading flight of the target and the initialization with no heading error. For comparison, the trajectories obtained when the interceptor uses PNG are also plotted. Since the target does not maneuver and there is no heading error, the trajectories coincide with those for the SMC guidance law with $\theta_r = 0$.

Figure 11 presents similar HO trajectories for the case in which the adversaries have equal speeds: i.e., $K = 1$. In such a case, based on Theorem 5, if the adversaries do not maneuver, then only HO is possible. It can be seen that using the proposed guidance law enables intercepting a target with a required intercept angle varying between -30 deg to 30 deg. Using PN guidance in such a case will result with an intercept angle of 0 deg that is the result of the initial collision course.

The trajectories for the case when the interceptor has a speed advantage ($K = 2$), are plotted in Fig. 12. Following Theorem 6 for

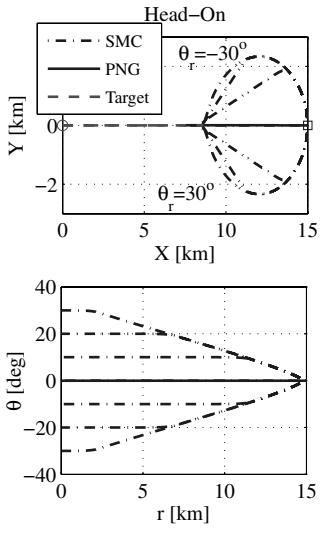

Fig. 11 Head-on trajectories; target does not maneuver; $K = 1$.

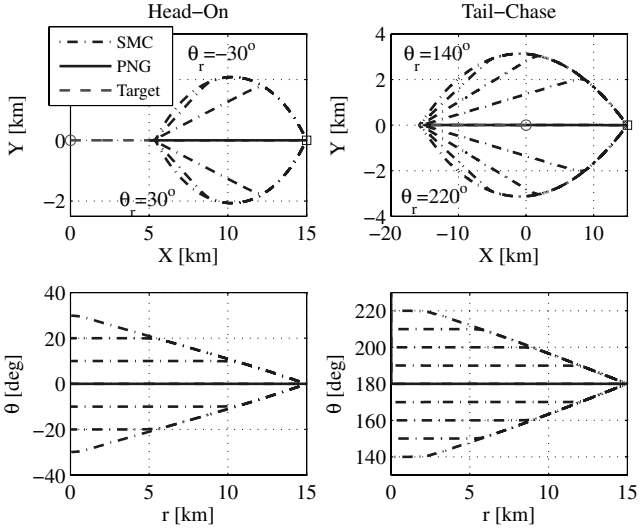

Fig. 12 Head-on and tail-chase trajectories; target does not maneuver; $K = 2$.

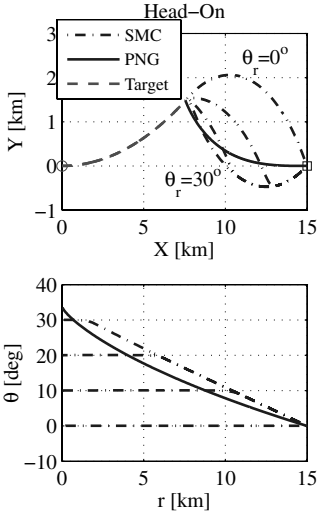

Fig. 14 Head-on trajectories; target maneuvers 5*g*; $K = 1$.

such a case, only head-on and tail-chase are feasible. It is apparent that in HO θ_r can vary between -30 to 30 deg, while for TC it can vary between -40 to 40 deg. As for $K < 1$ (Fig. 10) here too the increased interception range of θ_r can be attributed to the significantly longer duration that TC allows, due to the significantly lower closing speed (approximately 1000 m/s for TC compared to 3000 m/s in an HO scenario).

Remark 4: Although the proposed SMC guidance law allows a large range of intercept angles, this range is still limited. For example, for $K = 2$ we are unable to enforce TC with, say, $\theta_r = 120$ deg. This is due to the initialization of the engagement with $\theta = 180$ deg and the finite time nature of the missile interception engagement, terminating when $r = 0$ or $\dot{r} = 0$ (see Eq. (17)).

C. Constant Target Maneuver

In this subsection we investigate the case in which the target performs a constant maneuver of 5 *g*. Figures 13–15 present the trajectories for $K = 0.8$, 1, and 2, respectively. In all runs the LOS continuously rotates, due to the need to reach the required interception geometry in the face of the target maneuver. Nonetheless, the missile was able to maintain the required intercept angle θ_r after it was reached. Also, in all cases the missile was able to impose the required interception angle, with a very small miss distance that is less than 0.5 m, in the face of the constant target maneuver.

For the case in which the missile has a speed disadvantage ($K = 0.8$, see Fig. 13), HO and HP are feasible. Similar to the case of a nonmaneuvering target (Fig. 10), here too using HP allows a larger range of intercept angles θ_r compared to HO (θ_r can vary between -10 and 30 deg, compared to 0 to 20 deg in HO). As can be seen, PNG enables interception, but in both cases of initialization in HO and HP geometries, the trajectory converged to an HO engagement, with the angle θ varying throughout the engagement. It is also evident that in HP for $\theta_r = 0$, after an initial transient, the interceptor maintains the same trajectory as that of the target, while leading it.

Trajectories for $K = 1$ are plotted in Fig. 14. As for the nonmaneuvering-target case (Fig. 11), only HO engagement is feasible. Compared to Fig. 13 the increase in the speed of the interceptor allows a slightly larger range of intercept angles (a range of 0–30 deg, compared to 0–20 deg).

Figure 15 presents the trajectories for $K = 2$. As in the previous cases, HO enables a smaller range of interception angles compared to tail-chase. Comparing the results of HO to those of Figs. 13 and 14, the increased range of intercept angles, due to the increased interceptor speed, is evident. Note that for TC with $\theta_r = 180$ deg the interceptor joins and then follows the path of target. As in the previous cases, using PN guidance the intercept angle θ varies

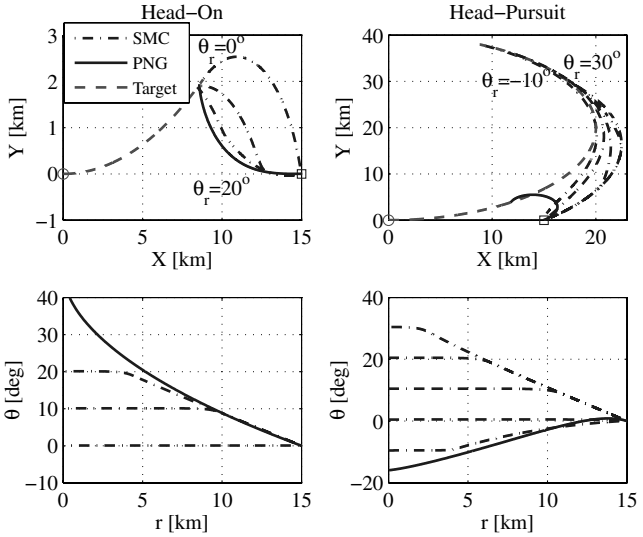

Fig. 13 Head-on and head-pursuit trajectories; target maneuvers 5*g*; $K = 0.8$.

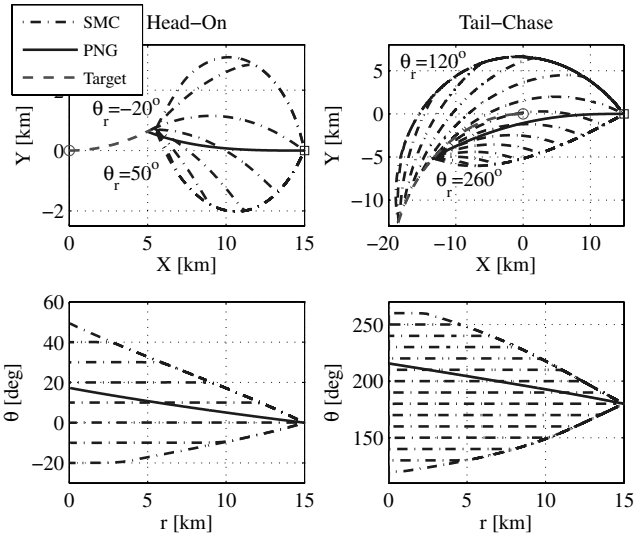

Fig. 15 Head-on and tail-chase trajectories; target maneuvers 5*g*; $K = 2$.

throughout the engagement and is dependent on all the scenario parameters and initial conditions.

VII. Conclusions

A new guidance concept that enables imposing a predetermined intercept angle relative to a maneuvering target's flight direction was presented. The guidance law can be applied in head-on, tail-chase, and the novel head-pursuit engagement.

The proposed guidance concept was implemented using the sliding-mode approach. The controller allows bringing the system to a sliding surface that imposes the required geometric rule. Simulation results confirmed that this surface can be reached and maintained in the face of target maneuvers and large initial deviation from the required intercept geometry. In contrast, when using proportional navigation guidance, the intercept geometry may vary throughout the engagement and is dependent on all the scenario parameters and initial conditions.

In deriving the proposed guidance law the common assumption of flight along an initial collision triangle was not taken. Thus, the guidance law is applicable for both the midcourse and endgame phases of an interception engagement. A unique feature of the guidance law is that the required intercept geometry is enforced from early on in the scenario, and not just at intercept. This may be advantageous from observability considerations (in noise-corrupted scenarios) and from counter-countermeasures considerations.

Simulation results also showed that head-on is the hardest scenario to obtain a required interception geometry and it places on the interceptor the most severe maneuverability requirement. Thus, in cases in which it is essential to impose a predetermined interception angle, tail-chase or head-pursuit engagements should be considered instead. The choice between the two is dependent on the speed ratio of the adversaries, as head-pursuit can be maintained when the interceptor has a speed disadvantage, while tail-chase requires a speed advantage by the interceptor.

References

[1] Shima, T., and Golan, O., "Head Pursuit Guidance," *Journal of Guidance, Control, and Dynamics*, Vol. 30, No. 5, 2007, pp. 1437–1444. doi:10.2514/1.27737

[2] Zarchan, P., *Tactical and Strategic Missile Guidance*, Vol. 176, Progress in Astronautics and Aeronautics, AIAA, Washington, D.C., 1997.

[3] Bryson, E. A., and Ho, C. Y., *Applied Optimal Control*, Blaisdell, Waltham, MA, 1969.

[4] Yuan, L., "Homing and Navigational Courses of Automatic Target-Seeking Devices," *Journal of Applied Physics*, Vol. 19, No. 12, 1948, pp. 1122–1128. doi:10.1063/1.1715028

[5] Shneydor, N. A., *Missile Guidance and Pursuit—Kinematics, Dynamics and Control*, Series in Engineering Science, Horwood, Chichester, England, U.K., 1998.

[6] Bruckstein, A. M., "Why the Ants Trails Look so Straight and Nice," *The Mathematical Intelligencer*, Vol. 15, No. 2, 1993, pp. 59–62. doi:10.1007/BF03024195

[7] Kim, B. S., Lee, J. G., and Han, H. S., "Biased PNG Law for Impact with Angular Constraint," *IEEE Transactions on Aerospace and Electronic Systems*, Vol. 34, No. 1, 1999, pp. 277–288. doi:10.1109/7.640285

[8] Ratnoo, A., and Ghose, D., "Impact Angle Constrained Interception of Stationary Targets," *Journal of Guidance, Control, and Dynamics*, Vol. 31, No. 6, 2008, pp. 1816–1821. doi:10.2514/1.37864

[9] Kim, M., and Grider, K. V., "Terminal Guidance for Impact Attitude Angle Constrained Flight Trajectories," *IEEE Transactions on Aerospace and Electronic Systems*, Vol. AES-9, No. 6, 1973, pp. 852–859. doi:10.1109/TAES.1973.309659

[10] Song, T. L., Shin, S. J., and Cho, H., "Impact Angle Control for Planar Engagements," *IEEE Transactions on Aerospace and Electronic Systems*, Vol. 35, No. 4, 1999, pp. 1439–1444. doi:10.1109/7.805460

[11] Ryoo, C. K., Cho, H., and Tahk, M. J., "Optimal Guidance Laws with Terminal Impact Angle Constraint," *Journal of Guidance, Control, and Dynamics*, Vol. 28, No. 4, 2005, pp. 724–732. doi:10.2514/1.8392

[12] Ryoo, C. K., Cho, H., and Tahk, M. J., "Time-to-Go Weighted Optimal Guidance with Impact Angle Constraints," *IEEE Transactions on Control Systems Technology*, Vol. 14, No. 3, 2006, pp. 483–492. doi:10.1109/TCST.2006.872525

[13] Cherry, G., "A General Explicit, Optimizing Guidance Law for Rocket-Propelled Spaceflight," AIAA Astrodynamics, Guidance, and Control Conference, AIAA Paper 64-638, 1964.

[14] Ohlmeyer, E., and Phillips, C., "Generalized Vector Explicit Guidance," *Journal of Guidance, Control, and Dynamics*, Vol. 29, No. 2, 2006, pp. 261–268. doi:10.2514/1.14956

[15] Manchester, I., and Savkin, A. V., "Circular Navigation Missile Guidance with Incomplete Information and Uncertain Autopilot Model," *Journal of Guidance, Control, and Dynamics*, Vol. 27, No. 6, 2004, pp. 1078–1083. doi:10.2514/1.3371

[16] Idan, M., Golan, O., and Guelman, M., "Optimal Planar Interception with Terminal Constraints," *Journal of Guidance, Control, and Dynamics*, Vol. 18, No. 6, 1995, pp. 1273–1279. doi:10.2514/3.21541

[17] Ariff, O., Zbikowski, R., Tsourdos, A., and White, B., "Differential Geometric Guidance Based on the Involute of the Target's Trajectory," *Journal of Guidance, Control, and Dynamics*, Vol. 28, No. 5, 2005, pp. 990–996. doi:10.2514/1.11041

[18] Shaferman, V., and Shima, T., "Linear Quadratic Guidance Laws for Imposing a Terminal Intercept Angle," *Journal of Guidance, Control, and Dynamics*, Vol. 31, No. 5, 2008, pp. 1400–1412. doi:10.2514/1.32836

[19] Ratnoo, A., and Ghose, D., "State-Dependent Riccati-Equation-Based Guidance Law for Impact-Angle-Constrained Trajectories," *Journal of Guidance, Control, and Dynamics*, Vol. 32, No. 1, 2009, pp. 320–325. doi:10.2514/1.37876

[20] Utkin, V. I., "Variable Structure Systems with Sliding Modes," *IEEE Transactions on Automatic Control*, Vol. 22, No. 2, 1977, pp. 212–222. doi:10.1109/TAC.1977.1101446

[21] Moon, J., Kim, K., and Kim, Y., "Design of Missile Guidance Law Via Variable Structure Control," *Journal of Guidance, Control, and Dynamics*, Vol. 24, No. 4, 2001, pp. 659–664. doi:10.2514/2.4792

[22] Zhou, D., Mu, C., and Xu, W., "Adaptive Sliding-Mode Guidance of a Homing Missile," *Journal of Guidance, Control, and Dynamics*, Vol. 22, No. 4, 1999, pp. 589–594. doi:10.2514/2.4421

[23] Shtessel, Y., Shkolnikov, I., and Levant, A., "Smooth Second-Order Sliding Modes: Missile Guidance Application," *Automatica*, Vol. 43, No. 8, 2007, pp. 1470–1476. doi:10.1016/j.automatica.2007.01.008

[24] Shima, T., Idan, M., and Golan, O., "Sliding-Mode Control for Integrated Missile Autopilot Guidance," *Journal of Guidance, Control, and Dynamics*, Vol. 29, No. 2, 2006, pp. 250–260. doi:10.2514/1.14951

[25] Idan, M., Shima, T., and Golan, O., "Integrated Sliding Mode Autopilot-Guidance for Dual-Control Missiles," *Journal of Guidance, Control, and Dynamics*, Vol. 30, No. 4, 2007, pp. 1081–1089. doi:10.2514/1.24953

[26] Shtessel, Y., and Tournes, C., "Integrated Higher-Order Sliding Mode Guidance and Autopilot for Dual-Control Missiles," *Journal of Guidance, Control, and Dynamics*, Vol. 32, No. 1, 2009, pp. 79–94. doi:10.2514/1.36961

[27] Shima, T., and Golan, O., "Exo-Atmospheric Guidance of an Accelerating Interceptor Missile," AIAA Guidance, Navigation, and Control Conference, AIAA Paper 2008-6494, 2008.

[28] Slotine, J.-J. E., and Li, W., *Applied Nonlinear Control*, chap. 7, Prentice–Hall, Upper Saddle River, NJ, 1991, pp. 276–307.

[29] Levant, A., "Higher-Order Sliding Modes, Differential and Output-Feedback Control," *International Journal of Control*, Vol. 76, No. 9–10, 2003, pp. 924–941. doi:10.1080/0020717031000099029

[30] Shtessel, Y., Shkolnikov, I., and Brown, M., "An Asymptotic Second Order Smooth Sliding Mode Control," *Asian Journal of Control*, Vol. 4, No. 5, 2003, pp. 498–504.